Density Diagnostics for EIS

P.R. Young, CCLRC/RAL

This document contains a reference list of recommended density diagnostics for users of the *EUV Imaging Spectrograph* (EIS) on board Solar-B. EIS observing studies will require choosing spectral windows focussed on the particular science that is to be accomplished. Thus a given study may only have one or two diagnostics and so it is important to have an understanding of which diagnostics will be useful in different conditions.

The table below lists the main diagnostics available to EIS, arranged by temperature of formation of the ion. A crude rating is also given indicating how useful the ratios are. The page number refers to the page of the document where the ion is discussed. The Appendix (p. 10) gives a full list of all the transitions discussed in this document, together with the EIS effective area at each wavelength.

Ion	Ratio	Page	log T	log N_e	Rating	Comment
Si X	λ261.04/λ258.37	2	6.1	8.0–10.0	**	QS, AR
S X	λ196.81/λ264.23	3	6.1	8.0–10.0	*	AR, FL
Fe XII	λ186.9/λ195.1	6	6.2	8.0–12.0	***	QS, AR, FL
Fe XIII	λ203.8/λ202.0	7	6.2	8.5–10.5	****	QS, AR
	λ196.54/λ202.04	7	6.2	9.5–11.5	***	AR, FL
S XI	λ190.36/λ191.27	4	6.3	10.5–12.5	**	AR, FL
	λ285.82/λ281.40	4	6.3	8.0–10.0	**	AR
Fe XIV	λ264.79/λ274.20	8	6.3	9.0–11.0	***	AR
Ni XVI	λ194.02/λ185.23	9	6.4	9.5–11.5	*	AR, FL
Ar XIV	λ191.40/λ194.40	5	6.5	10.0–12.0	*	AR, FL

The notes below give further information relevant to this document.

- EIS-A is the 250–290 Å channel, EIS-B is the 170–210 Å channel.
- The effective area of EIS shows significant variations with wavelength, particularly in the EIS-B channel where it can vary by a factor 10 over 10 Å. 'Weak' lines close to the peak of the EIS-B effective area function can thus end up being stronger than 'strong' lines at the edges of the bandpass. This is important for some of the lines of low abundance elements (S, Ar, Ni) listed in this document that lie in the high effective area 190–200 Å region.

Si X, log Tmax=6.1

The density sensitivity of the λ261.04/λ258.37 ratio is directly comparable with that of the λ356.0/λ347.4 ratio that has been successfully used for many years with SOHO/CDS. It is ideal for both quiet Sun and active region conditions (densities 10^8–10^{10} cm^{-3}). Neither line is affected by blending to any significant degree. The only drawback is the low sensitivity of the ratio, it only varying by just over a factor 3.

RECOMMENDATION: the best of the 'cool corona' density diagnostics in normal quiet Sun and active region conditions.

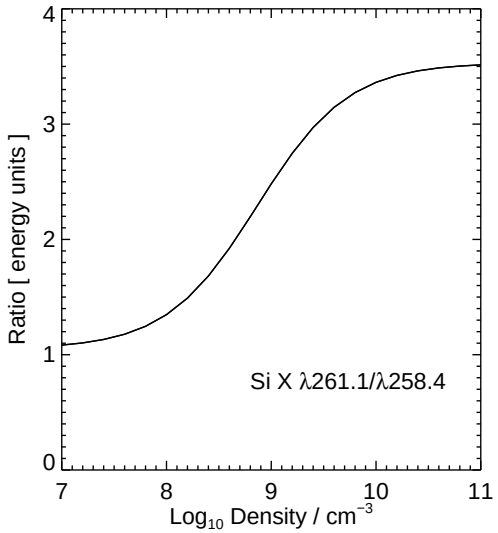

Figure 1: Si X λ261.1/λ258.4 density diagnostic.

S X, log Tmax=6.1

The λ196.81/λ264.23 ratio shows good density sensitivity, particularly above 10^{10} cm^{-3} and, despite the relatively large wavelength separation, there is little temperature sensitivity.

Note that, although the emissivity of the S X λ180.73 line is more than 5 times higher than the λ196.8 line, the effective area at 196.8 Å is 15 times greater, and so this is preferred.

The λ264.2 line will not be affected by blending, but the λ196 line is predicted to be partially blended with the Fe XII λ196.87 line. Given the uncertainties in the Fe XII atomic model, this blend will have to be studied with EIS spectra to determine how significant this blend is.

RECOMMENDATION: useful for looking at high densities in the cool corona during flares, but Fe XII blend for λ196.8 line needs to be checked.

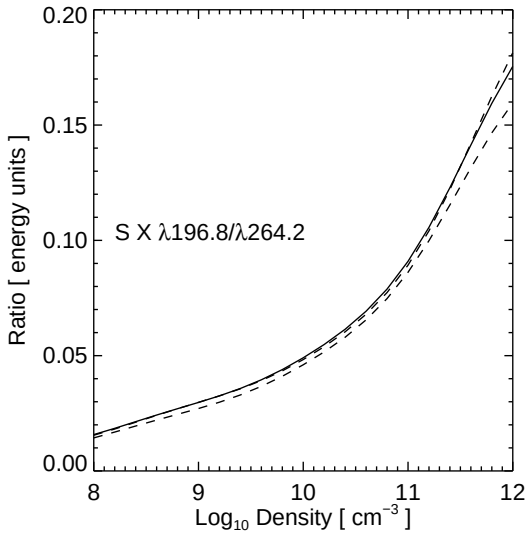

Figure 2: S X λ196.8/λ264.2 density diagnostic. The dashed lines show the density sensitivity at temperatures log $T_{\max} \pm 0.15$.

S XI, log Tmax=6.3

The λ190.36/λ191.27 ratio involves two unblended lines, close in wavelength and with high effective areas. However, the ratio is only sensitive at high densities ($> 10^{10}$ cm^{-3}), and so will only be useful for flaring active regions.

The λ285.8/λ281.4 is sensitive to lower densities and will be useful for normal active region observations, or off-limb. The Fe XIII λ203.8/λ202.0 or Fe XIV λ274/λ264 ratios are to be preferred, though, as they involve stronger lines with higher effective areas.

RECOMMENDATION: λ190.36/λ191.27 is a good flare diagnostic.

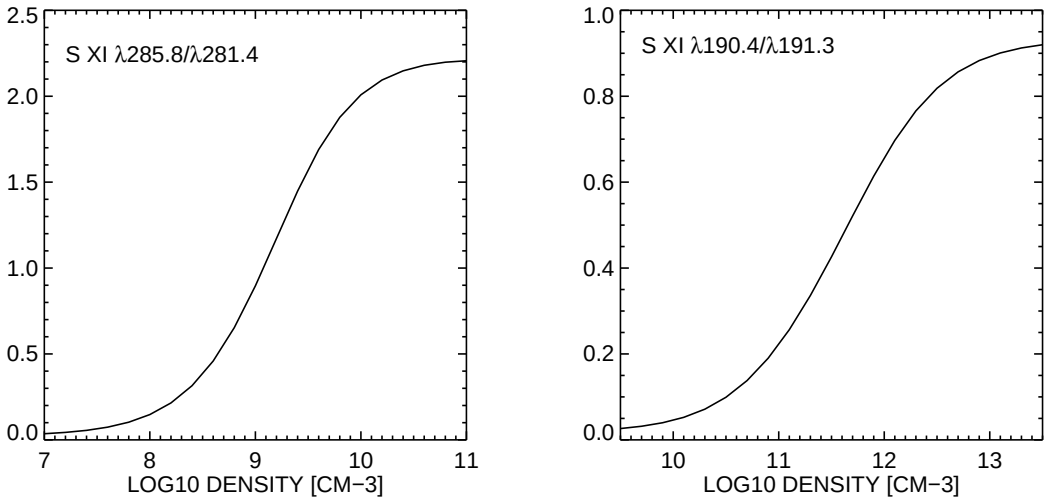

Figure 3: S XI density diagnostics.

Ar XIV, log Tmax=6.5

The λ187.97/λ194.40 ratio is a very good density diagnostic, sensitive to densities in the range 10^{10}–10^{12} cm^{-3}. However, the λ187.97 line is expected to become dominated by the Fe XXI λ187.92 line in flare conditions.

An alternative diagnostic is λ191.40/λ194.40 which is less sensitive but has no blending problems. The high effective areas at the locations of these two lines balance the weakness of the lines due to the low abundance of argon.

RECOMMENDATION: the only good density diagnostic at these temperatures. λ191.40/λ194.40 is recommended due to blending problems with λ187.97/λ194.40 during flares.

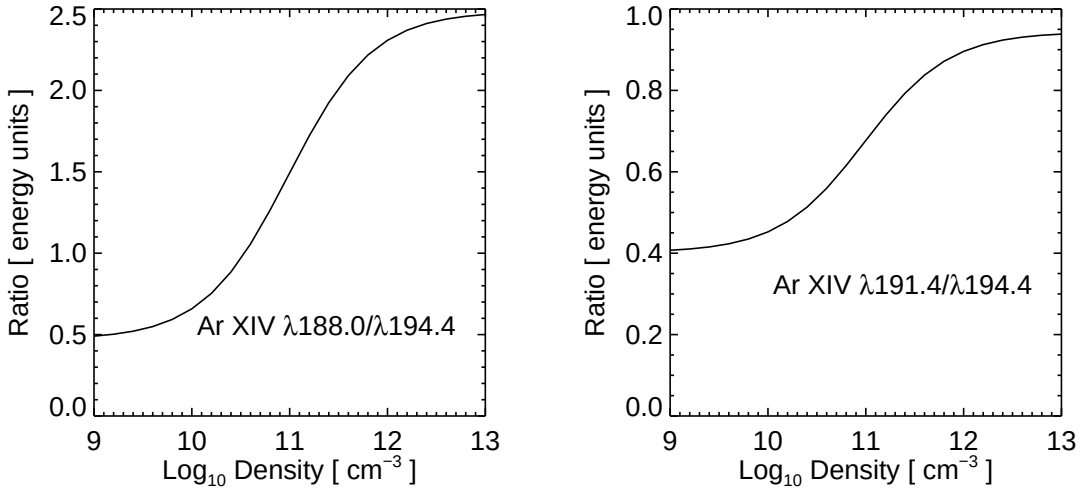

Figure 4: Ar XIV density diagnostic.

Fe XII, log Tmax=6.2

The λ186.9/λ195.1 ratio shows strong sensitivity over a wide density range (4 orders of magnitude). The λ195.1 lies right at the top of the effective area curve for EIS-B and will be strongest EIS line in most solar conditions. The λ186.9 line is a blend of two Fe XII lines of comparable strength, but is also partly blended with a S XI line, but this should not contribute more than 10 % and, given the close temperatures of formation of the two ions, will not vary significantly with temperature.

NOTE: the Fe XII atomic data has been significantly revised recently. The plot shown was made with the older data currently in CHIANTI v4.2. The ratio may change with the new data.

RECOMMENDATION: The λ186.9/λ195.1 ratio is an excellent density diagnostic involving strong lines. However sensitivity in 'quiet' conditions ($8.5 \leq \log N_{\rm e} \leq 9.5$) is lower than at high densities, and there is a blend with S XI.

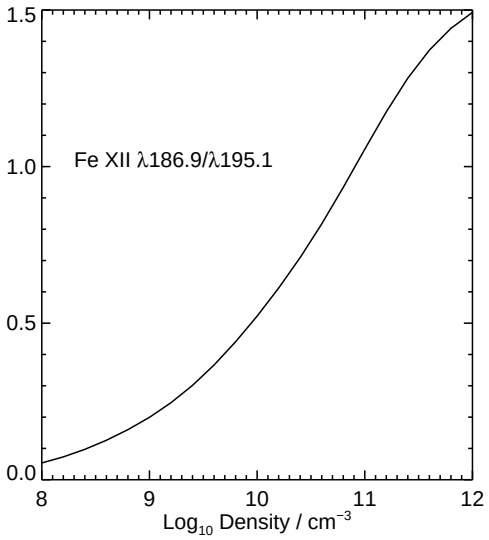

Figure 5: Fe XII density diagnostic.

Fe XIII, log Tmax=6.2

The λ203.8/λ202.0 ratio is one of the best density diagnostics in the EUV due to the close proximity of the lines, their strength, and their high sensitivity (the ratio varies by over a factor 40). The only disadvantage for EIS is that the effective area is varying very sharply over this wavelength region: from 0.070 cm^2 to 0.037 cm^2 between the two lines. Thus it will be critical to assess the accuracy of the calibration in this region through density insensitive line ratios. Note that the λ203.8 line is a blend of two Fe XIII lines with wavelengths 203.80 and 203.83 Å.

Another very useful diagnostic is to take λ196.54/λ202.04 which is also very sensitive, but to higher densities ($> 10^{9.5}$ cm^{-3}). The effective area at 196.5 Å is high (0.26 cm^2), aiding measurement in lower density conditions.

RECOMMENDATION: λ203.8/λ202.0 is recommended for standard active regions, while λ196.5/λ202.0 will be valuable for flaring plasma.

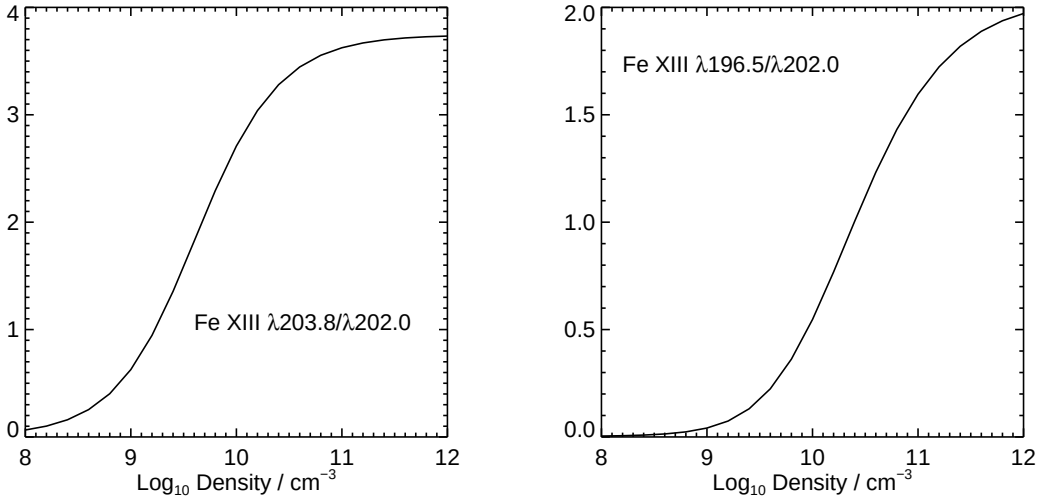

Figure 6: Fe XIII density diagnostics.

Fe XIV, log Tmax=6.3

Several Fe XIV lines are found in EIS-A, and the best diagnostic is λ264.79/λ274.20. The λ264 line is not affected by blending, but λ274 is blended with Si VII λ274.18, which would have some contribution in quiet conditions. If the Si VII λ275.35 line is measured (and this is likely since it is one of the stronger 'cool' lines in the spectrum), then some estimate of the Si VII contribution can be made since the λ274.18/λ275.35 ratio is ≤ 0.25 in all conditions.

RECOMMENDATION: λ264.79/λ274.20 is a good diagnostic for active regions. Users should be aware of the Si VII blend, however.

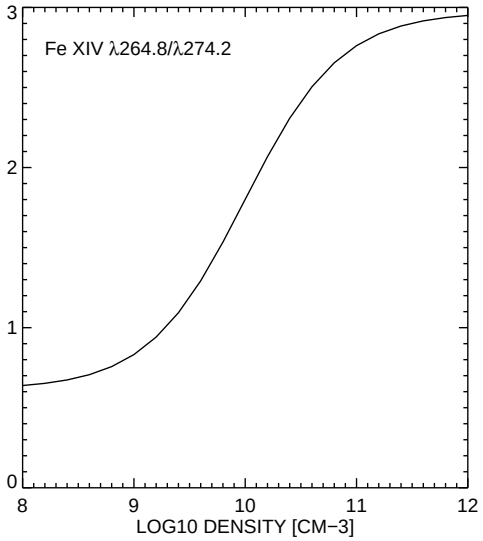

Figure 7: Fe XIV λ264.79/λ274.20 density diagnostic.

Ni XVI, log Tmax=6.4

Iso-electronic with Fe XIV, the density diagnostic equivalent of the well-known Fe XIV λ219/λ211 diagnostic (which is missed with EIS) for Ni XVI is λ194.02/λ185.23. There is also a line at λ195.28 related to λ185.2 by a branching ratio with value 0.234, but the effective areas are in the ratio 3.70, so there's not much to choose between the two. The λ195.28 line is very close to Fe XII and so there may be difficulty measuring the Ni XVI line except in very active conditions. The λ185.2 line will be blended with a Fe VIII line in some conditions, but Ni XVI should dominate for strong active regions.

RECOMMENDATION: the low abundance of Ni coupled with possible blends will make the Ni XVI line difficult to use in most conditions, but λ194.02/λ185.23 is potentially a good diagnostic in flare conditions.

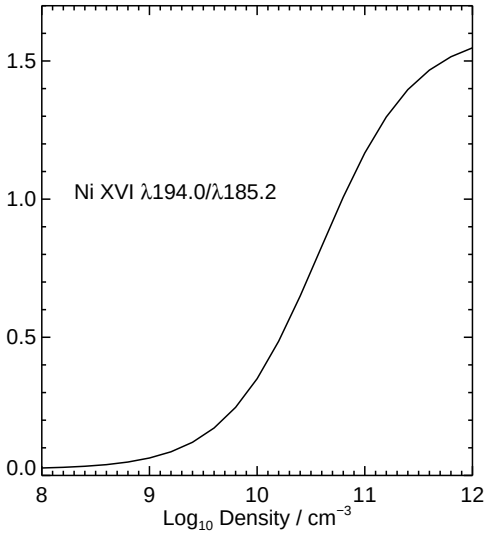

Figure 8: Ni XVI density diagnostic.

Appendix: transitions and effective areas

The table below gives the transitions discussed in this document and the EIS effective areas at their wavelengths. The wavelength and transition information are from v4.2 of the CHIANTI database while the effective areas are derived from EIS software in Solarsoft (extracted Dec 2004).

Ion	Transition	λ/Å	EA/mm^2
Si X	$2s^2\ 2p\ ^2P_{3/2}$ - $2s\ 2p^2\ ^2P_{3/2}$	258.37	5.0
	$2s^2\ 2p\ ^2P_{3/2}$ - $2s\ 2p^2\ ^2P_{1/2}$	261.04	5.9
S X	$2s^2\ 2p^3\ ^2D_{5/2}$ - $2s\ 2p^4\ ^2P_{3/2}$	180.73	1.6
	$2s^2\ 2p^3\ ^2P_{3/2}$ - $2s\ 2p^4\ ^2P_{3/2}$	196.81	25.5
	$2s^2\ 2p^3\ ^4S_{3/2}$ - $2s\ 2p^4\ ^4P_{5/2}$	264.23	7.1
S XI	$2s^2\ 2p^2\ ^1D_2$ - $2s\ 2p^3\ ^1P_1$	190.36	17.5
	$2s^2\ 2p^2\ ^3P_2$ - $2s\ 2p^3\ ^3S_1$	191.27	19.5
	$2s^2\ 2p^2\ ^3P_0$ - $2s\ 2p^3\ ^3D_1$	281.40	4.2
	$2s^2\ 2p^2\ ^3P_1$ - $2s\ 2p^3\ ^3D_1$	285.59	2.7
	$2s^2\ 2p^2\ ^3P_1$ - $2s\ 2p^3\ ^3D_2$	285.82	2.6
Ar XIV	$2s^2\ 2p\ ^2P_{3/2}$ - $2s\ 2p^2\ ^2P_{3/2}$	187.97	12.1
	$2s^2\ 2p\ ^2P_{3/2}$ - $2s\ 2p^2\ ^2P_{1/2}$	191.40	19.8
	$2s^2\ 2p\ ^2P_{1/2}$ - $2s\ 2p^2\ ^2S_{1/2}$	194.40	25.2
Fe XII	$3s^2\ 3p^3\ ^2D_{5/2}$ - $3s^2\ 3p^2\ (^3P)\ 3d\ ^2F_{7/2}$	186.89	9.9
	$3s^2\ 3p^3\ ^2D_{3/2}$ - $3s^2\ 3p^2\ (^1D)\ 3d\ ^2D_{3/2}$	195.13	25.9
Fe XIII	$3s^2\ 3p^2\ ^1D_2$ - $3s^2\ 3p\ 3d\ ^1F_3$	196.54	25.8
	$3s^2\ 3p^2\ ^3P_0$ - $3s^2\ 3p\ 3d\ ^3P_1$	202.04	7.0
	$3s^2\ 3p^2\ ^3P_2$ - $3s^2\ 3p\ 3d\ ^3D_3$	203.82	3.7
Fe XIV	$3s^2\ 3p\ ^2P_{3/2}$ - $3s\ 3p^2\ ^2P_{3/2}$	264.78	7.3
	$3s^2\ 3p\ ^2P_{1/2}$ - $3s\ 3p^2\ ^2S_{1/2}$	274.20	7.8
Ni XVI	$3s^2\ 3p\ ^2P_{1/2}$ - $3s^2\ 3d\ ^2D_{3/2}$	185.23	6.7
	$3s^2\ 3p\ ^2P_{3/2}$ - $3s^2\ 3d\ ^2D_{5/2}$	194.02	24.7
	$3s^2\ 3p\ ^2P_{3/2}$ - $3s^2\ 3d\ ^2D_{3/2}$	195.28	25.9